Development of Robust Fractional-Order Controllers to Provide Effective Economic Load Dispatch Management in Interconnected Area Networks

J. Okoronkwo, A. Mati, Y. Jibril, G. Olarinoye, and A. S. Abubakar

1 Introduction

The integration of renewable energy sources into the grid affects the dynamic operation, as well as the response of the power system-to-system disturbances in terms of change in power flow patterns and sensitivity of the system to faults. Thus reducing frequency and tie-line power deviation within accepted operating standard in multiple areas of interconnected power systems is paramount. Load frequency controller (LFC) and automatic voltage regulator (AVR) play an important role in maintaining steady frequency and voltage to ensure reliability of electric power systems (Kroposki et al., 2017) (Grigsby, 2017). Load frequency control is one of the functions of automatic generation control (AGC) (Soundarrajan et al., 2012). The present challenge is in situations when there are integrated power systems of two or more areas with cascading multiple disturbances.

2 Theoretical Background

When considering renewable energy systems and other energy systems to be integrated in a multi-area interconnected microgrid power system, limiting frequency fluctuation by compensating for the deviation between generation and demand is optimal, (Khooban et al., 2018; Lal et al., 2018). This functionality and capability are often referred to as load frequency control (LFC). The load frequency control

J. Okoronkwo (✉) · A. Mati · Y. Jibril · G. Olarinoye · A. S. Abubakar
Department of Electrical Engineering, Ahmadu Bello University, Zaria, Kaduna State, Nigeria

A. O. Ayeni et al. (eds.), *Advanced Manufacturing in Biological, Petroleum, and Nanotechnology Processing*, Green Energy and Technology,
https://doi.org/10.1007/978-3-030-95820-6_26

(LFC) is to sustain and maintain system frequency of each area and tie-line power flow between areas during normal operating situations and variations in load demands (Chidambaram & Paramasivam, 2013; Lal et al., 2018). A functional LFC can not only guarantee the frequency stability of the MG but also increase its fuel saving efficiency (Khooban et al., 2018). To improve the response of LFC, many controllers including conventional PID control (Khooban et al., 2018), intelligent control (Bevrani et al., 2012), adaptive control (Xu et al., 2018), robust control (Liao & Xu, 2018), and MPC control (Ersdal et al., 2016) have been applied to the DGs of MAIMGs (Khooban et al., 2018).

The MG's low inertia capability compared to the grid remains a challenge maintaining the active and reactive power balances between the supply and utilization (Khooban et al., 2018), especially in the presence of intermittent RES and frequent load variations (Roslan et al., 2019). Few works have been carried out to address frequency control of isolated MG power systems; however, interconnected MG systems have not received much attention (Bevrani et al., 2012; Cau et al., 2014; Khooban et al., 2018).

Since the operating conditions of the LFC can change instantaneously (Khooban et al., 2018), the controller tuned for nominal conditions cannot work properly when exposed to other conditions. The performance of the controller primarily depends on its parameters; effective optimization of these parameters can play a controlling role and significant impact in promoting the output performance of the LFC control. So, to solve this problem, the control parameters were tuned according to the setoff point (Abdulkhader et al., 2018; Khooban et al., 2018).

As a measure of conformity to the control performance standards, a first compliance factor knows as ACE (area control error) is applied to the power system operations (Bevrani & Hiyama, 2017). To match the dynamic economic dispatch to load, system operators pick out trajectories of the generation units repeatedly or resort to manual outputs (Ross & Kim, 1980). The economic dispatch function provides set economic exponentials for the generation units. The tie schedules combine to obtain the net optimal AGC response tracks desired by unit generation as requirements for all units on AGC over the economic trajectories (Ross & Kim, 1980).

3 Material and Methods

3.1 Materials

The materials used for the research work are discussed in this subsection. They include all hardware and software used for the implementation and realization of the set objectives.

3.1.1 Hardware Platform

The research is simulated on a Dell laptop with specifications (operating system, Microsoft Windows 10; processor, 1.7 GHz Intel Core i5; memory, 4 GB 1600 MHz DDR3).

3.1.2 Software Platform

MATLAB ("MATrix LABoratory") software is used throughout this work for performing modeling, mathematical computations, algorithm development, and simulations.

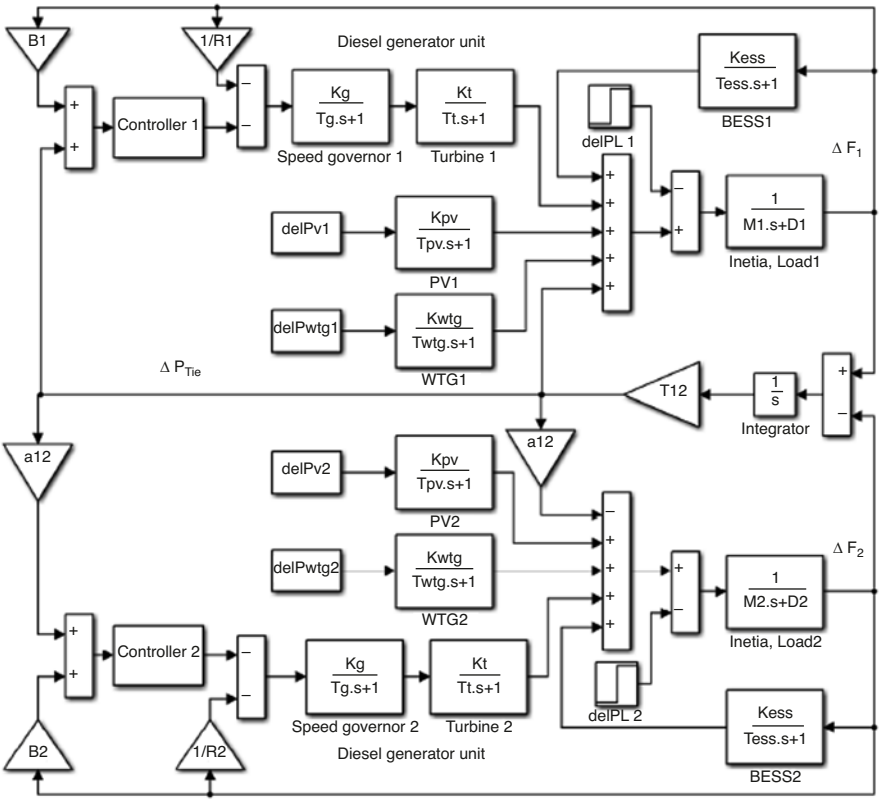

Fig. 1 Block diagram of two-area interconnected microgrid system. (Lal et al., 2018)

3.2 Methods

The steps of the methodology used in achieving the set objectives are as follows:

3.2.1 Two-Area Interconnected Microgrid Power System

The schematic diagram of a two-area interconnected microgrid network using energy generation units illustrated in Fig. 1 was implemented in MATLAB Simulink.

3.3 Performance Criteria for Optimization-Based Tuning of Controller Parameters

The controller parameters were optimized using the IAE, ITAE, ISE, and ITSE performance criteria, and the performance criteria are defined in Eqs. 1, 2, 3, 4, 5, 6, 7, 8 and 9:

$$J = \text{IAE} = \int_{t=0}^{t_{\text{sim}}} \left(\left|\Delta F_1\right| + \left|\Delta F_2\right| + \left|\Delta P_{\text{tie}}\right| \right) dt \tag{1}$$

$$J = \text{ITAE} = \int_{t=0}^{t_{\text{sim}}} t \left(\left|\Delta F_1\right| + \left|\Delta F_2\right| + \left|\Delta P_{tie}\right| \right) dt \tag{2}$$

$$J = \text{ISE} = \int_{t=0}^{t_{\text{sim}}} \left(\Delta F_1^2 + \Delta F_2^2 + \Delta P_{\text{tie}}^2 \right) dt \tag{3}$$

$$J = \text{ITSE} = \int_{t=0}^{t_{\text{sim}}} t \left(\Delta F_1^2 + \Delta F_2^2 + \Delta P_{\text{tie}}^2 \right) dt \tag{4}$$

where ΔF_1 and ΔF_2 are the system frequency deviations of areas 1 and 2, respectively (Lal & Barisal, 2019); ΔP_{tie} is the incremental change in tie-line power; and t is the simulation time. Hence, the optimization problem is stated as (Chen et al., 2019):

$$Minimize J \tag{5}$$

subject to

$$\left.\begin{aligned} K_P^{\min} \le K_P \le K_P^{\max} \\ K_I^{\min} \le K_I \le K_I^{\max} \\ K_D^{\min} \le K_D \le K_D^{\max} \end{aligned}\right\} \text{for PID controller} \tag{6}$$

$$\left.\begin{aligned} K_1^{\min} \le K_1 \le K_1^{\max} \\ K_2^{\min} \le K_2 \le K_2^{\max} \\ K_3^{\min} \le K_3 \le K_3^{\max} \\ K_4^{\min} \le K_4 \le K_4^{\max} \end{aligned}\right\} \text{for fuzzy } PID \text{ controller} \tag{7}$$

$$\left.\begin{aligned} K_P^{\min} \le K_P \le K_P^{\max} \\ K_I^{\min} \le K_I \le K_I^{\max} \\ K_D^{\min} \le K_D \le K_D^{\max} \\ \lambda_{\min} \le \lambda \le \lambda_{\max} \\ \mu_{\min} \le \mu \le \mu_{\max} \end{aligned}\right\} \text{for FOPID controller} \tag{8}$$

$$\left.\begin{aligned} K_1^{\min} \le K_1 \le K_1^{\max} \\ K_2^{\min} \le K_2 \le K_2^{\max} \\ K_3^{\min} \le K_3 \le K_3^{\max} \\ K_4^{\min} \le K_4 \le K_4^{\max} \\ \lambda_{\min} \le \lambda \le \lambda_{\max} \\ \mu_{\min} \le \mu \le \mu_{\max} \end{aligned}\right\} \text{for fuzzy FOPID controller} \tag{9}$$

where K_1, K_2, K_3, K_4, K_P, K_I, K_D are the controller gains and λ, μ are fractional order of the FOPID controller. These are independent variables which need to be optimally selected in order to control the load frequency of the system.

4 Results and Discussion

The fuzzy logic good performance attained in specific member functions was enhanced by the introduction of the FOPID controller to avoid the need for additional retuning or online auto-tuning, even in unstable cases (Pan & Das, 2016). The FOPID controller also shows high robustness properties concerning parameter variation in nonlinear rate constraint on feedback elements and on disconnection of some components (Pan & Das, 2012). The FOPID controllers offer very good robustness, and the performance does not degrade appreciably even when there are changes in system parameters (Pan & Das, 2016). The ruggedness of the FOPID controller in the feedback loop is evident because it consistently keeps the controller gains especially ISE at lower values compared to PID and fuzzy PID structures. The

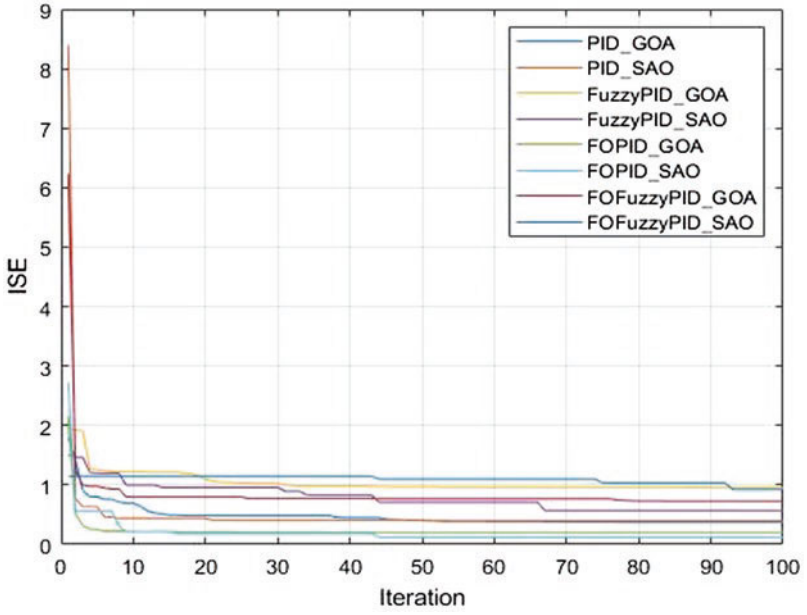

Fig. 2 Convergence plot of ISE criterion

robust features are due to the use of gain margin, phase margin, and iso-damping property. The parameters of the controllers were optimized using the grasshopper optimization algorithm and smell agent optimization as described above. The ISE, IAE, ITSE, and ITAE performance criteria were utilized in the optimization process. Each of the performance criteria was applied to different controllers, and a comparison of their performances was carried out to determine the best performing criterion. The ISE performance criterion was found to be the best performing (Kocaarslan & Çam, 2005) (Figs. 2 and 3, Table 1).

Four performance criteria were used to develop the controllers for this work. The results obtained for the IAE performance criterion are shown in Table 2; the FOPID controller outperformed other controllers with a minimum fitness value of 18.2555 when optimized with the SAO, followed by the fuzzy PID controller optimized with the GOA with a minimum fitness value of 27.0761 as shown in Figs. 4 and 5. In Fig. 4, the controllers converge to values less than 100 after the first ten iterations, but after the 60th iteration, they all converge to stable values less than 50. This shows that the worst IAE criterion fitness value was obtained from the FO fuzzy PID controller optimized with SAO. The results also show that the performance of PID and FO fuzzy controllers was generally poor when optimized for the IAE criterion.

The results obtained for the ITSE performance criterion are shown in Table 3; the FOPID controller outperformed other controllers with minimum fitness values of 0.0325 and 0.089336 when optimized with the GOA and SAO, respectively. This is

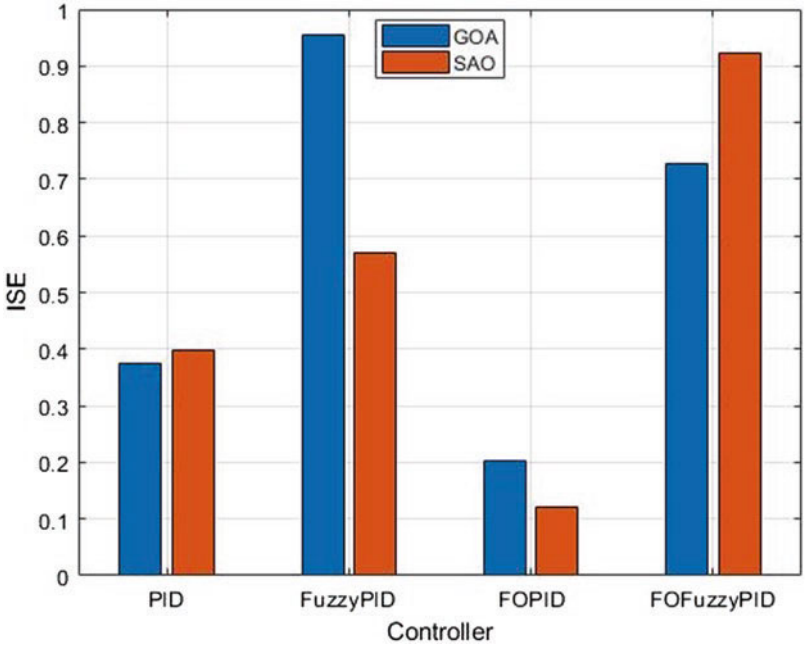

Fig. 3 Optimal fitness values of ISE criterion

Table 1 Optimal fitness values of ISE performance criterion

Controller structure	Optimization algorithm	ISE
PID	GOA	0.37474
	SAO	0.3981
Fuzzy PID	GOA	0.95426
	SAO	0.57044
FOPID	GOA	0.2034
	SAO	0.1215
FO fuzzy PID	GOA	0.7276
	SAO	0.92324

shown in Fig. 6 similar to previous convergence plots of Fig. 4; this converges to values between 0 and 0.5 after five iterations. The worst fitness value was obtained from the fuzzy PID controller optimized with GOA. The results also show that the performance of fuzzy controllers was generally poor when optimized for the ITSE criterion especially using GOA (Fig. 7).

The results obtained for the ITAE performance criterion are shown in Table 4; the fuzzy FOPID controller outperformed other controllers with minimum fitness values of 12.213 and 13.3172 when optimized with the SAO and GOA, respectively, as shown in Figs. 8 and 9. The signals in Fig. 8 converge to values between 0 and 50

Table 2 Optimal fitness values of IAE performance criterion

Controller structure	Optimization algorithm	IAE
PID	GOA	35.0241
	SAO	36.0429
Fuzzy PID	GOA	27.0761
	SAO	24.5477
FOPID	GOA	29.9658
	SAO	18.2555
FO fuzzy PID	GOA	37.852
	SAO	33.5883

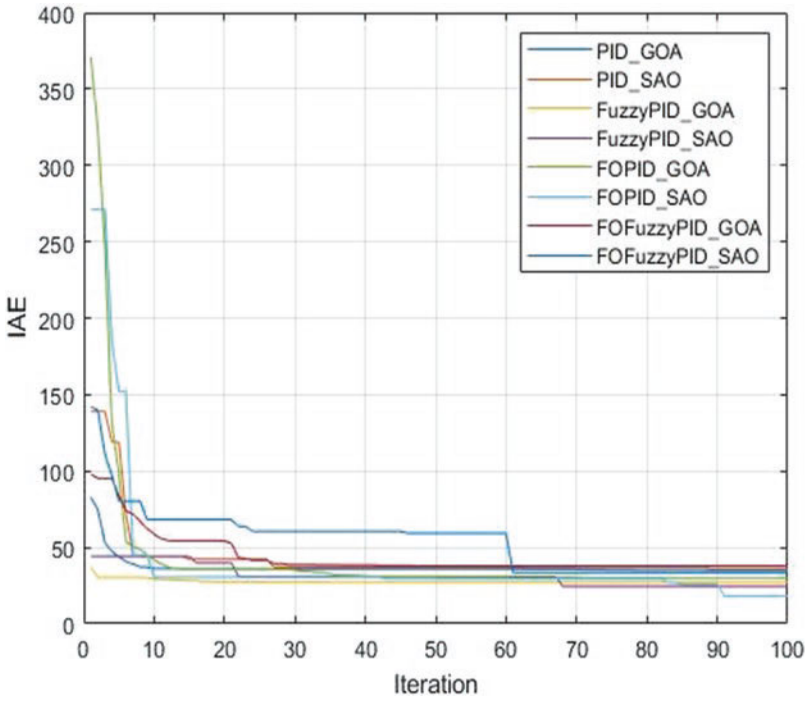

Fig. 4 Convergence plot of IAE criterion

after 30 iterations. The worst fitness value was obtained from the FO fuzzy PID controller optimized with GOA as the convergence pattern takes the form of an exponentially decaying function. The results also show that the performance of PID controllers was generally poor when optimized for the ITAE criterion especially using GOA.

In summary, the performance of developed FOPID and fuzzy FOPID controllers was compared with basic PID and fuzzy PID controllers using the convergence

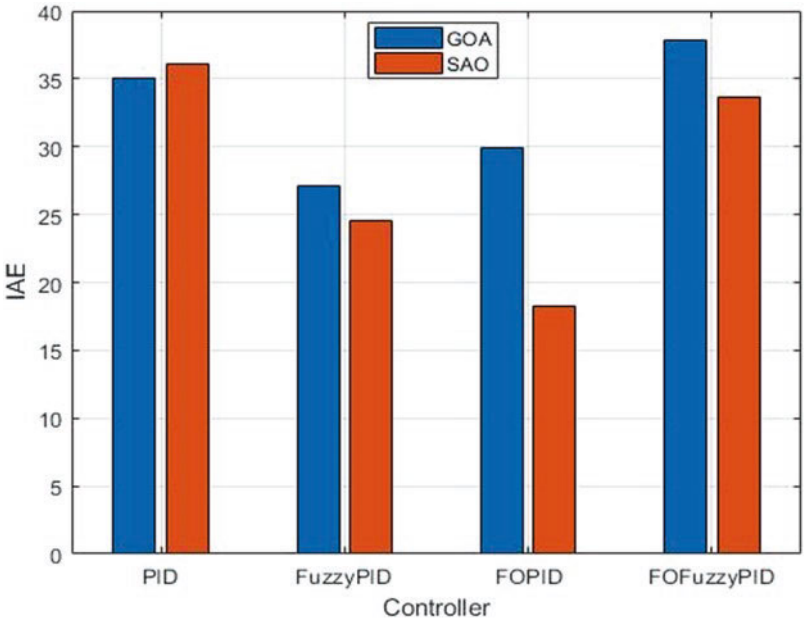

Fig. 5 Optimal fitness values of IAE criterion

Table 3 Optimal fitness values of ITSE performance criterion

Controller structure	Optimization algorithm	ITSE
PID	GOA	0.13694
	SAO	0.1586
Fuzzy PID	GOA	0.34457
	SAO	0.092525
FOPID	GOA	0.0325
	SAO	0.089336
FO fuzzy PID	GOA	0.27617
	SAO	0.22589

characteristics and optimal fitness values of performance criteria. The results obtained showed that the FOPID controller outperformed other controllers as shown along with the optimal fitness values of the ITSE performance criterion. This is evident that the developed controller is able to match the dynamic dispatch of the economic generation to load relating to load management between control areas.

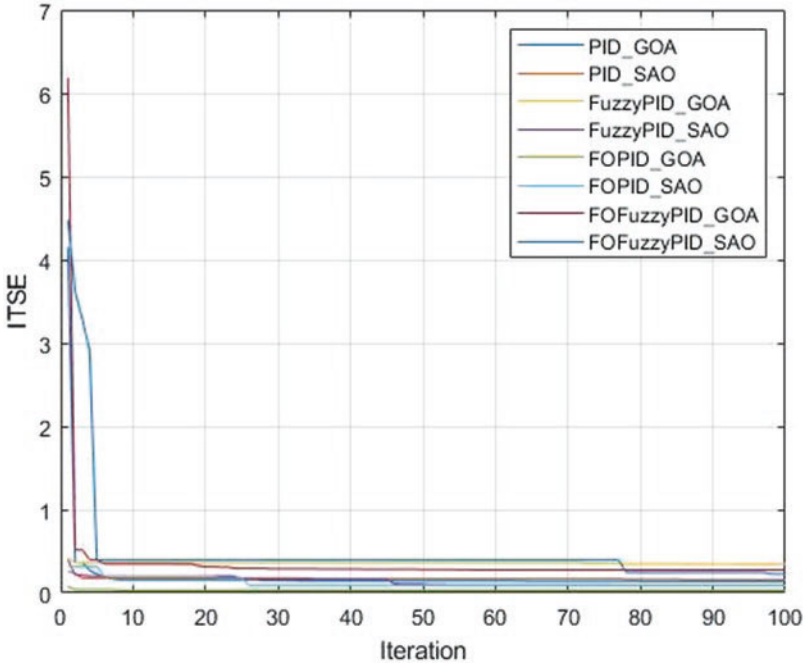

Fig. 6 Convergence plot of ITSE criterion

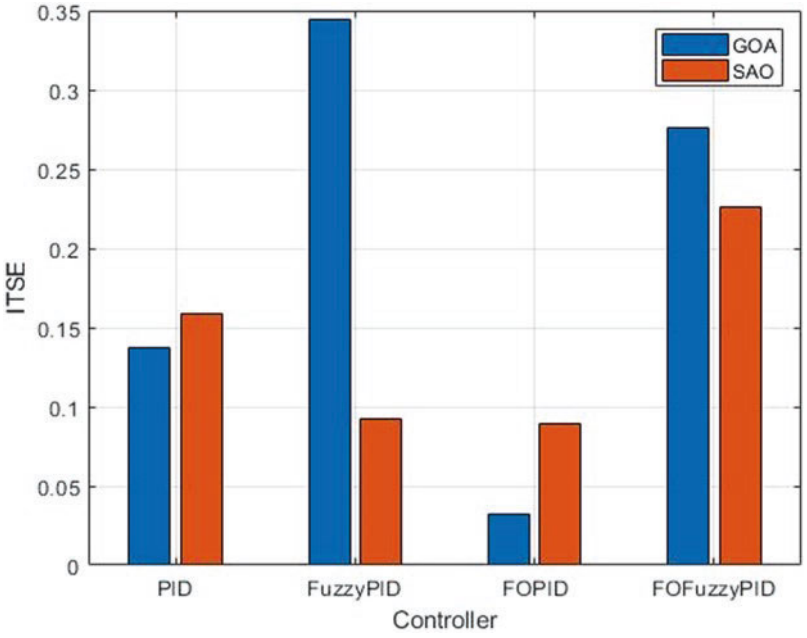

Fig. 7 Optimal fitness values of ITSE criterion

Table 4 Optimal fitness values of ITAE performance criterion

Controller structure	Optimization algorithm	ITAE
PID	GOA	40.5866
	SAO	42.8153
Fuzzy PID	GOA	13.3172
	SAO	12.213
FOPID	GOA	23.3432
	SAO	23.105
FO fuzzy PID	GOA	56.1118
	SAO	23.0759

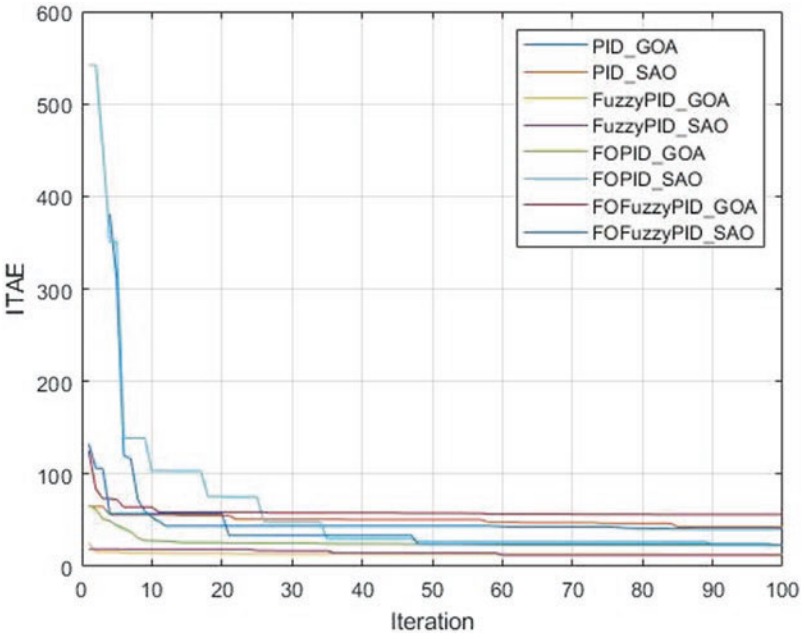

Fig. 8 Convergence plot of ITAE criterion

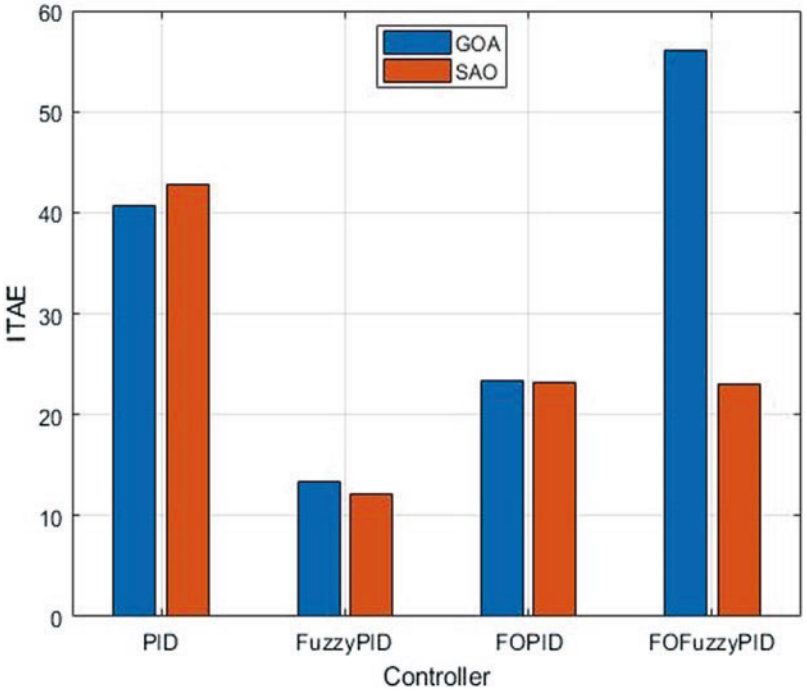

Fig. 9 Optimal fitness values of ITAE criterion

References

Abdulkhader, H. K., Jacob, J., & Mathew, A. T. (2018). Fractional-order lead-lag compensator-based multi-band power system stabiliser design using a hybrid dynamic GA-PSO algorithm. *IET Generation, Transmission & Distribution, 12*(13), 3248–3260. https://doi.org/10.1049/iet-gtd.2017.1087

Bevrani, H., & Hiyama, T. (2017). *Intelligent automatic generation control*. CRC Press.

Bevrani, H., Habibi, F., Babahajyani, P., Watanabe, M., & Mitani, Y. (2012). Intelligent Frequency Control in an AC Microgrid: Online PSO-Based Fuzzy Tuning Approach. *IEEE Transactions on Smart Grid, 3*(4), 1935–1944. https://doi.org/10.1109/TSG.2012.2196806

Cau, G., Cocco, D., Petrollese, M., Knudsen Kær, S., & Milan, C. (2014). Energy management strategy based on short-term generation scheduling for a renewable microgrid using a hydrogen storage system. *Energy Conversion and Management, 87*, 820–831. https://doi.org/10.1016/j.enconman.2014.07.078

Chen, G., Li, Z., Zhang, Z., & Li, S. (2019). An improved ACO algorithm optimized fuzzy PID controller for load frequency control in multi area interconnected power systems. *IEEE Access, 8*, 6429–6447.

Chidambaram, I. A., & Paramasivam, B. (2013). Optimized load-frequency simulation in restructured power system with Redox Flow Batteries and Interline Power Flow Controller. *International Journal of Electrical Power & Energy Systems, 50*, 9–24. https://doi.org/10.1016/j.ijepes.2013.02.004

Ersdal, A. M., Imsland, L., & Uhlen, K. (2016). Model predictive load-frequency control. *IEEE Transactions on Power Systems, 31*(1), 777–785. https://doi.org/10.1109/TPWRS.2015.2412614

Grigsby, L. L. (2017). *Power system stability and control*. CRC Press.

Khooban, M., Niknam, T., Shasadeghi, M., Dragicevic, T., & Blaabjerg, F. (2018). Load frequency control in microgrids based on a stochastic noninteger controller. *IEEE Transactions on Sustainable Energy, 9*(2), 853–861. https://doi.org/10.1109/TSTE.2017.2763607

Kocaarslan, I., & Çam, E. (2005). Fuzzy logic controller in interconnected electrical power systems for load-frequency control. *International Journal of Electrical Power & Energy Systems, 27*(8), 542–549.

Kroposki, B., Johnson, B., Zhang, Y., Gevorgian, V., Denholm, P., Hodge, B., & Hannegan, B. (2017). Achieving a 100% renewable grid: Operating electric power systems with extremely high levels of variable renewable energy. *IEEE Power and Energy Magazine, 15*(2), 61–73. https://doi.org/10.1109/MPE.2016.2637122

Lal, D. K., & Barisal, A. K. (2019). Combined load frequency and terminal voltage control of power systems using moth flame optimization algorithm. *Journal of Electrical Systems and Information Technology, 6*(1), 1–24.

Lal, D. K., Barisal, A. K., & Tripathy, M. (2018). Load frequency control of multi area interconnected microgrid power system using grasshopper optimization algorithm optimized fuzzy PID controller. *2018 Recent Advances on Engineering, Technology and Computational Sciences (RAETCS)*, 1–6. https://doi.org/10.1109/RAETCS.2018.8443847

Liao, K., & Xu, Y. (2018). A robust load frequency control scheme for power systems based on second-order sliding mode and extended disturbance observer. *IEEE Transactions on Industrial Informatics, 14*(7), 3076–3086. https://doi.org/10.1109/TII.2017.2771487

Pan, I., & Das, S. (2012). *Intelligent fractional order systems and control: An introduction* (Vol. 438). Springer.

Pan, I., & Das, S. (2016). Fractional order fuzzy control of hybrid power system with renewable generation using chaotic PSO. *ISA Transactions, 62*, 19–29. https://doi.org/10.1016/j.isatra.2015.03.003

Roslan, M. F., Hannan, M. A., Ker, P. J., & Uddin, M. N. (2019). Microgrid control methods toward achieving sustainable energy management. *Applied Energy, 240*, 583–607. https://doi.org/10.1016/j.apenergy.2019.02.070

Ross, D. W., & Kim, S. (1980). Dynamic economic dispatch of generation. *IEEE Transactions on Power Apparatus and Systems, PAS-99*(6), 2060–2068. https://doi.org/10.1109/TPAS.1980.319847

Soundarrajan, A., Sumathi, S., & Sivamurugan, G. (2012). Voltage and frequency control in power generating system using hybrid evolutionary algorithms. *Journal of Vibration and Control, 18*(2), 214–227.

Xu, D., Liu, J., Yan, X., & Yan, W. (2018). A novel adaptive neural network constrained control for a multi-area interconnected power system with hybrid energy storage. *IEEE Transactions on Industrial Electronics, 65*(8), 6625–6634. https://doi.org/10.1109/TIE.2017.2767544